LBL-11806 c.2
Preprint

Lawrence Berkeley Laboratory
UNIVERSITY OF CALIFORNIA

Accelerator & Fusion Research Division

Submitted to Physical Review D

SCALING, MULTIPLICITY AND TEMPERATURE OF e^+e^- → HADRONS

T.F. Hoang and Bruce Cork

November 1980

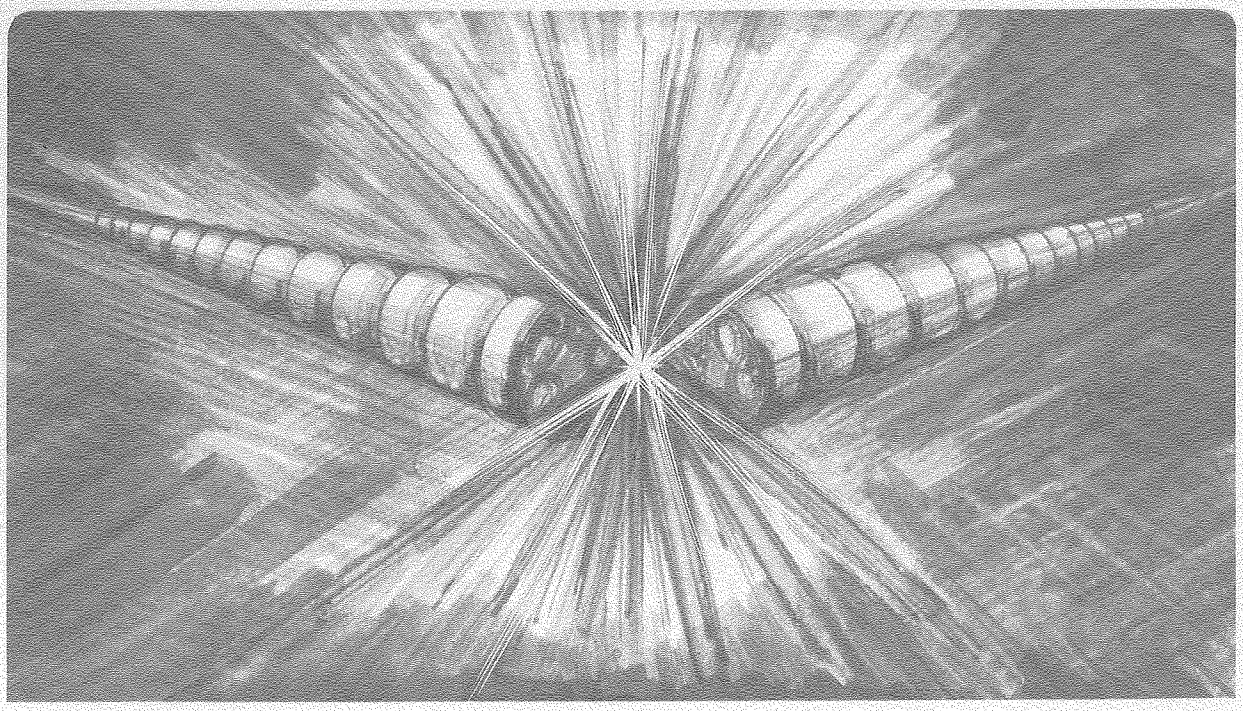

Prepared for the U.S. Department of Energy under Contract W-7405-ENG-48

DISCLAIMER

LBL-11806

Scaling, Multiplicity and Temperature of e^+e^- → hadrons

T.F. Hoang
1749 Oxford Street, Berkeley, CA 94709

and

Bruce Cork
Lawrence Berkeley Laboratory, Berkeley, CA 94720

Properties of meson production by e^+e^- annihilations for $E_{c.m.}$ = 3.0 to 31.2 GeV have been analyzed using the Bose-Einstein distribution modified for the Feynman-Yang scaling. Validity tests have been made with the P_T and P_L distributions measured with respect to the jet axis. The average charged multiplicity is found to follow an empirical power law $E_{c.m.}^{1/2}$. The temperatures deduced from $\langle P_T \rangle$ increase slowly with $E_{c.m.}$.

The scaling behavior is investigated in terms of the parameter $\lambda = 2\langle P_T \rangle / \pi \langle P_L \rangle$ used to modify the Bose-Einstein distribution. An anomaly resembling a phase transition of the specific heat of the hadronic matter is found at a temperature near 127 MeV corresponding to the threshold for Υ (9.5) production.

1. Introduction

Ever since the discovery of the J/ψ particle in 1974, many experiments have been carried out with colliding e^+e^- beams, aiming at detection of new particles. As a byproduct of these elaborate experiments, there has been accumulated a wealth of data on the meson production by e^+e^- annihilations

$$e^+e^- \to \text{hadrons}. \qquad (1)$$

The c.m. energies which have been explored to date extend beyond 31 GeV, thanks to the advent of the PETRA accelerator.

The characteristic features of the average multiplicity of charged mesons produced in (1) are as follows.[1] It increases faster than $\ell n\, s$ as has been observed at lower energies,[2] a behavior expected from various models,[3] in particular the parton model.[4] Yet, it remains far below the prediction by QCD (cf. infra). Since the behavior of the average multiplicity serves mostly as model testing, it is expedient to know if the experimental result can be accounted for by any other model, for instance Landau's hydrodynamical model.[5] In this regard, we note that the statistical model which predicts a linear dependence on the c.m. energy is ruled out by the data.[6]

Another remarkable property of reaction (1) is the jet structure,[7] a feature which is sui generis of the e^+e^- annihilation, and can be recognized without ambiguity by simple inspection in some events at PETRA energies. Thus, the transverse and the longitudinal momenta of a secondary meson from (1) are measured with respect to the jet axis, a situation different from the case of meson production by hadron-hadron collisions. A question arises: Is the Bose-Einstein type distribution modified for the Feynman-Yang scaling[8] still adequate to describe the P_T and P_L distributions thus measured?

The purpose of this paper is to present results of investigation on meson production by e^+e^- annihilation (1), and to discuss the temperature behavior deduced from the average P_T as well as an interesting property found in the scaling behavior in terms of the scaling parameter introduced to modify the Bose-Einstein distribution, namely an N-shaped anomaly near the T(9.5) threshold, resembling a phase transition.

2. Energy dependence of the average multiplicity

We begin with the average multiplicity $\langle n \rangle$ of the e^+e^- annihilation (1). Note that most experimental data deal with only charged pions and that a recent experiment at ADONE[9] finds the behavior of neutral secondaries similar to that for charged ones for $E_{c.m.}$ = 1.4 to 2.9 GeV. Consider, therefore, the data of the charged multiplicity from ADONE, SPEAR, DASP, PLUTO and TASSO[9-10] as shown in Fig. 1. Clearly, the data show an upward curvature; this trend rules out the ℓns dependence of the multiplicity, as mentioned before.

Next, let us compare the data with the prediction by QCD according to which we expect[11]

$$\langle n_{ch} \rangle = f(E_{c.m.}/\Lambda)/f(E_o/\Lambda) \tag{2}$$

where

$$f(E_{c.m.}/\Lambda) = \exp[e\sqrt{\frac{N_c}{\pi b}\,\ell n(E^2_{c.m.}/\Lambda^2)}] \tag{3}$$

with $b = (11 - 2N_f/3)/4\pi$; $N_c = 3$ and $N_f = 4$ are numbers of color and flavor, respectively; $\Lambda \cong 0.5$ GeV and $E_o \cong 1$ GeV are fixed constants.[12] This prediction is characterized by the abrupt rise of $\langle n_{ch} \rangle$ with $E_{c.m.}$ which deviates very far from the experimental data. More specifically, the fit (not shown) requires the parameter $\sqrt{b}$ to be increased by a factor ~ 1.74, corresponding

to an effective strong coupling constant $\alpha_s = 1/b\ell n\ (E_{c.m.}/\Lambda)$ about 3 times larger than the value predicted by QCD for short distances.

We now turn to Landau's hydrodynamical model.[13] We note that its application to the case of e^+e^- annihilation has already been discussed by various authors.[5] The essential point is this: if the volume in which the energy is distributed is constant as in the case of e^+e^- annihilation, then the average multiplicity is expected to be

$$\langle n \rangle \sim E_{c.m.}^{1/(1+c_s^2)} \tag{4}$$

where c_s is the sound velocity (in units of $c = 1$). We see that if $c_s = 1$, as for scaling violation, Ref. 5(b), then $\langle n \rangle \sim E_{c.m.}^{1/2}$ as Landau's original prediction for nucleon-nucleon collisions. However, we emphasize that the physics contents of the two cases are quite different; see footnote 14.

Therefore, we are led to try the following empirical law for the charged multiplicity of reaction (1)

$$\langle n_{ch} \rangle = a \cdot E_{c.m.}^{1/2} + b \tag{5}$$

a and b being two parameters to be determined by fitting the experimental data. By least-squares fit we find

$$a = 2.04 \pm 0.04, \quad b = 0.15 \pm 0.43.$$

The fit is shown by the solid line in Fig. 1. A comparison with the experimental points indicates that apart from $E_{c.m.} < 2.5$ GeV, the fit is in general satisfactory.[15] We note that the estimate of b is consistent with zero, as should be under the assumption of a photon gas, and that our fit agrees with that of the JADE collaboration,[16] using the Fermi model to fit their data.

3. The P_T and P_L distributions

In the investigation of meson production using Landau's hydrodynamical model, it has been found that in the case of hadron-hadron collisions as well as $\bar{p}p$ annihilation,[17] the general properties of the transverse and longitudinal momentum, P_T and P_L, can be described, gross modo, by the following Bose-Einstein distribution modified to account for scaling

$$\frac{d\sigma}{d^3p} \sim \frac{1}{e^{\varepsilon(\lambda)/T}-1} \tag{6}$$

where

$$\varepsilon(\lambda) = (P_T^2+\lambda^2 P_L^2+m^2)^{1/2}, \tag{7}$$

m being the mass of the produced meson under consideration. The two parameters are the temperature T and the scaling parameter λ. Note that, for simplicity, we have set both the Boltzmann constant k and the velocity of light c equal to unity, and that we shall return later to discuss the scaling properties of the parameter λ, in Sec. 5. Here, we have to test the validity of this distribution (6) for e^+e^- annihilations (1), using P_T and P_L measured with respect to the axis of two jets. We refer to Appendix I for another test of (6).

Consider first the P_T distribution. We recall that it is the same as that obtained from the original Bose-Einstein distribution, see Ref. 8(d),

$$\frac{d\sigma}{dp_T^2} \propto m_T K_2(m_T/T) \tag{8}$$

where m_T describes the transverse mass

$$m_T = \sqrt{P_T^2+m^2} \tag{9}$$

and K_2 is the modified Bessel function of the 2^d kind. Noting that

$K_2(x) \propto (\pi/2x)^{1/2} e^{-x}$, we may approximate (8) as

$$\frac{d\sigma}{dP_T^2} \propto \sqrt{m_T} \cdot e^{-m_T/T} \tag{10}$$

Thus the plot of the log of $d\sigma/dP_T^2$ divided by $\sqrt{m_T}$ vs. m_T should be linear.

We shall make use of the SPEAR data at $E_{c.m.} = 7.0\text{-}7.8$ GeV.[18] The result is shown in Fig. 2; the straight line represents the least-squares fit. A comparison of the experimental points with the fit indicates that the test is very satisfactory. From the slope of the fit, we deduce the temperature T = 135 ±3 to be compared with 122 MeV estimated from $\langle P_T \rangle$ of the PLUTO data at $E_{c.m.} = 7.7$ GeV, as shown in Fig. 5, the χ^2/point being 1.38.

As for the P_L distribution, we note that for $\lambda P_L >> m_T$, we may write

$$\frac{d\sigma}{dP_L} \propto e^{-P_L/\langle P_L \rangle} \tag{11}$$

the value of $\langle P_L \rangle$ being related to $\langle P_T \rangle$ as follows:

$$\langle P_T \rangle / \langle P_L \rangle = (\pi/2)\lambda \tag{12}$$

For the derivation of these relations, we refer to Ref. 8(a).

In Fig. 3 we have reproduced the SPEAR data. Note that for clarity not all the data points are shown here. We have performed a fit for the Feynman variable $x = 2P_L/E_{c.m.} \geq 0.1$. The slope of the fit yields $\langle x \rangle = 0.184 \pm 0.014$. The fit as shown by the dashed line indicates that here again the test is rather satisfactory, with χ^2/point = 1.23.

4. The temperature behavior

As is well known from high energy reactions, the average transverse momentum

of produced mesons is limited. The measurements of $\langle P_T \rangle$ by the PLUTO and the TASSO collaborations[10] indicate a trend of a slow increase from $E_{c.m.} = 3$ to 31.2 GeV. To investigate this important property, it is more convenient to express $\langle P_T \rangle$ in terms of the temperature T, since the P_T distribution, Eq. (8), depends solely on the parameter T of the modified Bose-Einstein distribution.

According to (10), we find

$$\langle P_T \rangle = m\sqrt{\frac{\pi T}{2m}}\,\frac{K_{5/2}(m/T)}{K_2(m/T)} \,. \tag{13}$$

We have plotted in Fig. 4 the relationship between $\langle P_T \rangle$ and T for m = 140 MeV.

If we convert the values of $\langle P_T \rangle$ of the PLUTO and the TASSO collaborations into T (MeV), the results are shown in Fig. 5. We see that in the energy region up to 30 MeV, the temperature is certainly not constant, but rather increases with the c.m. energy.

In an attempt to investigate the energy dependence of T, we assume

$$T \propto E_{c.m.}^{\alpha} \tag{14}$$

We first make an overall fit to all the data as shown in Fig. 5 and find

$$\alpha = 0.30 \pm 0.06.$$

Next, for definiteness, we perform another fit with cut-offs to be discussed in Appendix II, and obtain

$$\alpha = 0.36 \pm 0.03 \qquad \text{for} \qquad 5 \leqslant E_{c.m.} < 20 \text{ GeV}.$$

From these fits, we conclude that $\alpha \neq 0$. This rules out the constancy of temperature, i.e. constant $\langle P_T \rangle$. However, it is clear that this behavior

(14) cannot hold for ever-increasing $E_{c.m.}$, because according to (13) this would lead to $\langle P_T \rangle \sim \sqrt{T}$, which is in contradiction with the property of limited $\langle P_T \rangle$ as mentioned earlier. It would be interesting to know when the turn-over of the behavior shown in Fig. 5 will take place, see Appendix II, Eq. (25).

5. The scaling behavior

We now turn to another characteristic feature of the meson production by e^+e^- annihilation, namely P_L scaling violation, a property in contrast with pp and other hadron-hadron collisions. We propose to investigate this important problem using the parameter λ of the modified Bose-Einstein distribution (6).

As is easily seen from (6), we expect $\langle P_L \rangle$ to be inversely proportional to λ; see Refs. 8(a) and 19. Thus, in the high energy limit, the Feynman-Yang scaling requires

$$\lambda\sqrt{s}/2 \to \text{const}, \tag{15}$$

this property has been found for pp collisions with $P_{lab} > 20$ GeV/c; see Ref. 8(b).

We have calculated the values of λ from the averages of P_T and P_L of the PLUTO and the TASSO collaborations,[10] use being made of Eq. (12). The values of $\lambda\sqrt{s}/2$ thus obtained are plotted in Fig. 6, the dashed line being arbitrarily drawn to guide the eye.

We note that $\lambda\sqrt{s}/2$ increases monotonically with the c.m. energies $\sqrt{s}$ = 3 to 27.4 GeV without reaching a constant value as is required by Feynman-Yang scaling. In this regard, it is interesting to note that in the context of the hydrodynamical model, the scaling violation of e^+e^- annihilation (1) is anticipated in the case of the limiting sound velocity $c_s = 1$, as has been pointed

out by Satz et al., Ref. 5(b). Another scaling will be discussed in Appendix I.

6. T(9.5) Threshold effect on the scaling

In an attempt to get more insight into the physical meaning of the scaling violation described in the previous section, we consider the plot of $1/\lambda$ against T, instead of against $\sqrt{s}$ as in Fig. 6. This amounts to a change of variables, which is motivated by the fact that $1/\lambda$ is related to the c.m. energy as is seen from (15).

The results are shown in Fig. 7. Note that only a few error bars are shown, because of clarity, whereas typical errors on T are about 5 MeV. The dashed curve is an arbitrary eyeball fit.

As an illustration, we have presented in the same figure, but with a different vertical scale, the case of $p+p \to \pi^- + \ldots$ for P_{lab} = 12 to 1600 GeV/c.[20] A comparison of these two plots indicates a striking difference in behavior between e^+e^- annihilation on the one hand, and pp collisions on the other hand.

We note that this difference is significant, in spite of scant data we have at our disposal. This is because of the following reasons. First, the point marked by 9.40 GeV represents the measurements "off the T-resonance", the "on resonance" point[21] namely at $E_{c.m.}$ = 9.46 GeV, corresponding to a point (not shown) at $1/\lambda = 2.26 \pm 0.09$ and $T = 134 \pm 4$ MeV, situated much lower than the 9,40 GeV point on the plot. Next, we have compared the portion of the curve in the region T = 100 to 120 MeV with that from the SLAC-LBL data[22] at $E_{c.m.}$ = 4.0 to 7.4 GeV and found the same trend of rise.

Now, this difference in scaling behavior between meson production by

e^+e^- annihilation on the one hand, and pp collision on the other, becomes even more striking if we compare the derivatives

$$C = \Delta(1/\lambda)/\Delta T \tag{16}$$

deduced from the two plots under consideration. The results thus obtained are shown in Fig. 8, the errors being shown by the shaded bands.

A comparison of the two plots indicates a sort of anomaly in the behavior of e^+e^- annihilation. Here, in contrast with its pp case, which shows a monotonical increase, we observe a drop in the region marked by AB, with a maximum at $T_{max} \cong 127$ MeV followed by a minimum at $T_{min} \cong 145$ MeV, which is comparable to the characteristic temperature, equal to the pion mass, as in Eq. (13), the uncertainties on these estimates being $\sim\pm 5$ MeV. Now, after the minimum, the trend of rise becomes quite similar to that of the pp case, indeed, both showing a sort of asymptotic behavior for the increasing temperature.

It is interesting to note that the estimated temperature at maximum, $T_{max} \cong 127$ MeV, turns out to be close to the threshold of $\Upsilon(9.5)$ production by e^+e^- annihilation, which is 134 ± 4 MeV according to the "on-resonance" measurement by the PLUTO collaboration,[21] as mentioned earlier. Note that the other thresholds for $\Upsilon'(10.0)$, $\Upsilon''(10.3)$ and $\Upsilon'''(10.6)$ are approximately $\Delta T = 2$ MeV apart from each other.

Thus, we are led to tentatively interpret the sudden drop observed in the C-T plot of Fig. 8 for the e^+e^- annihilation as related to the $b\bar{b}$ production. Now, the spin-parity of $\Upsilon(9.5)$ is 1^-, its decay into two photon-like gluons is strictly forbidden, whereas the three-gluon decay

$$\Upsilon \to g + g + g \tag{17}$$

is allowed. This has been observed experimentally as three jets by the PLUTO collaboration,[23] with the following characteristics. First, the most probable configuration of the three-gluon jets corresponds to the case where two of them are emitted in the opposite direction of the third one, within a small angle;[24] consequently, the event looks like an asymmetric two-jet, "back to back" with broadened P_T. Another property of the three-jet from the $\Upsilon(9.5)$ decay is that the average of charge-multiplicity $\langle n_{ch} \rangle = 8.0 \pm 0.3$ is found to be greater than 6.3 ± 0.4 of genuine two-jet events, namely $e^+e^- \to q + \bar{q}$ at the same energy 9.5 GeV, yielding a smaller $\langle P_L \rangle$ which is $E_{c.m.}/\langle n_{ch} \rangle$. We therefore anticipate the values of $1/\lambda$ arising from the three-jet production to be in general less than those of two-jets. This effect accounts for the change in the behavior of $1/\lambda$ near $\Upsilon(9.5)$ threshold as observed in Fig. 7(a).

7. Remarks

From the above discussion, we should expect a similar effect near J/ψ production to occur at $T \cong 95$ MeV, since it is also a photon-like 1^- particle and its 3γ decay has been observed experimentally.[25] However, as the multiplicity in this case is much smaller, $\langle n_{ch} \rangle \cong 3.5$ and the jets are less collimated, the question arises whether the effect can actually be detected.

As regards the pp case, we note that the $\Upsilon(9.5)$ threshold occurs at $P_{lab} = 65.8$ GeV, corresponding to $T \cong 140$ MeV. But here, unlike the e^+e^- case, the production cross section is known to be rather small compared to the background, so that the signal to noise level may not be favorable for observing the effect as in the e^+e^- case.

Turning to plots of $C = \Delta(1/\lambda)/\Delta T$ against the temperature T in Fig. 8, we note the striking difference in the shape between the e^+e^- case and the

pp case. The question arises: What is the physical meaning of the quantity C defined in Eq. (16)? In this regard, we recall that in the case of scaling, we should expect $1/\lambda \sim E_{c.m.}$, as has been observed for π production by pp as well as $\pi^+ p$ and $K^+ p$ collisions.[26] It then follows that the derivative of $1/\lambda$ with respect to the temperature T, Eq. (16), may be regarded as the "specific heat" of hadronic matter created by either e^+e^- annihilation (1) or $pp \to \pi + \ldots$ collision. Thus, to a certain extent, the difference in the two plots of Fig. 8 bears some resemblance to that of specific heats of superconducting and ordinary alloys.[27] In other words, the sudden drop of the value C in the case of e^+e^- resembles a sort of "phase transition" of the hadronic matter constituted only by quarks and antiquarks of certain flavors. On the contrary, in the pp case there is always an excess of valence quarks in addition to the produced quark-antiquark pairs. It would be interesting to investigate the $\Upsilon(9.5)$ threshold effect in $\bar{p}p$ colliding beam experiments, which may have more resemblance to the e^+e^- case from the scaling point of view,[28] notwithstanding this difference, that the intermediate state of this case is not a virtual photon as in the case of e^+e^- annihilation.

Finally, it should be mentioned that from theoretical point of view, the possibility of a phase transition in hadronic matter produced in high energy reactions has been discussed by various authors on general grounds[32] and also within the framework of QCD.[33] It is deemed a challenge to any bona fide model of reaction (1) to account for, in particular, the anomaly of the behavior of the scaling parameter λ determined by experimental values of $\langle P_T \rangle$ and $\langle P_L \rangle$, an anomaly bearing striking resemblance with a phase transition as has been discussed in the present work.

Acknowledgments

The authors wish to thank Professors G. Chew, G. Hanson, C. Goegel, I.R. Hagedorn, I. Hinchliffe, A. Barbero-Galtieri, T. O'Halloran, R. Thun, and G. Trilling for many illuminating comments and stimulating discussion. One of the authors (TFH) acknowledges the Tsi-Jung Fund for continuous support. The work of another author (BC) was supported in part by the High Energy and Nuclear Physics Division of the U.S. Department of Energy under Contract W-7405-ENG-48.

Appendix I

We discuss an external consistency test of the modified Bose-Einstein distribution, Eq. (6), using the average of the total energy, $\langle E \rangle$, of the secondary mesons from the e^+e^- annihilation (1). It should be mentioned that, in the literature, the ratio of $\langle E \rangle / (E_{c.m.}/2)$ is referred to as the "radial scaling", and that its actual meaning differs somewhat from the Feynman-Yang scaling.[29]

We note that in the relativistic approximation, Eq. (7) becomes

$$\varepsilon(\lambda) = E - (1-\lambda)P_L \quad . \tag{18}$$

Thus, we find from (6) by neglecting the pion mass:

$$\langle E \rangle = \frac{2(1+\lambda+\lambda^2)}{\lambda(1+\lambda)} T \tag{19}$$

Note that for $\lambda = 1$, i.e. in the rest frame, $\langle E^* \rangle = 3T^*$ is the average energy in the relativistic case with $m = 0$.

With this expression, we have computed $\langle E \rangle$ for $E_{c.m.} = 3$ to 30 GeV using interpolated values of the temperature T and the scaling parameters λ from experiments of the PLUTO and the TASSO collaborations,[10] as shown in Figs. 5 and 6. The results thus obtained are shown in Fig. 9. Note that if there is radial scaling, the ratio $\langle E_{ch} \rangle / (E_{c.m.}/2)$ is independent of the c.m. energy, as has been observed in pp collisions.[30]

As for the test, we have used the values of $\langle E_{ch} \rangle / E_{c.m.}$ and the average charged multiplicity of the SLAC-LBL experiments.[31] The results are represented by the open circles in the same figure. A comparison with the curve indicates that the test is satisfactory, especially because the parameters T and λ used for the curve are taken from other experiments at PETRA as mentioned above.

Appendix II

In an attempt to avoid any ambiguity which may occur to the determination of the jet axis, we have limited ourselves to $\langle P_T \rangle$ data in the region $5 \leqslant E_{c.m.} < 20$ GeV.[34] The lower limit is so chosen that $\langle n_{ch} \rangle$ exceeds 4 (see Fig. 1). Consequently, each axis of the two back-to-back jets arising from e^+e^- annihilation into a quark-antiquark pair is determined by at least two observed particles.

As for the upper limit $E_{c.m.} < 20$ GeV, it is chosen to avoid eventual 3-jet events due to gluon emission by a quark or antiquark $e^+e^- \to q\bar{q}g$ emission observed at high energy by PETRA experiments,[35] amounting to $\sim$15% for $E_{c.m.} > 20$ GeV. In this case, the estimate of the average transverse momentum becomes more involved than the 2-jet case without gluon emission.

We now investigate how $\langle P_T \rangle$ is affected by gluon emission. For this purpose, consider the symmetric momentum tensor of the second order formed with the momenta p^i of hadrons from reaction (1):

$$T_{\alpha\beta} = \sum_i (\delta_{\alpha\beta}(p^i)^2 - p^i_\alpha p^i_\beta) \qquad (20)$$

$\alpha,\beta = 1, 2,$ and 3 and the summation is extended over all particles, charged as well as neutral. In this regard, we note that if there is thermal equilibrium among emitted particles as has been observed in hadron-hadron collisions,[36] then it is sufficient to consider only charged particles in the summation of (20).

As is well known, in the case of the inertia tensor, $T_{\alpha\beta}$ can be reduced to its diagonal form with real eigen values such that $\lambda_1 \geqslant \lambda_2 \geqslant \lambda_3$, following the usual convention.[37] Let $\vec{n}_1$, $\vec{n}_2$ and $\vec{n}_3$ be the corresponding eigen vectors,

namely the principal axes of the momentum ellipsoid (20) being chosen to be n_3 along which is P_L. Thus, for the two components of P_T we must have

$$\Sigma_i \vec{n}_1 \cdot \vec{p}_1^{\,i} = 0, \qquad \Sigma_i \vec{n}_2 \cdot \vec{p}_2^{\,i} = 0 \tag{21}$$

However, it is altogether not clear that these necessary conditions are actually satisfied by minimizing $\Sigma_i p_T^{\,2}$, a condition sometimes used inter alia to diagonalize the momentum ellipsoid (20).

The components $\vec{n}_1 \cdot \vec{p}_1^{\,i}$ and $\vec{n}_2 \cdot \vec{p}_2^{\,i}$ are referred to as "out" and "in" the event plane defined by n_2 and n_3, respectively.[38] With this notation, we have

$$\langle P_T^{\,2} \rangle = \langle (P_T^{\,2})_{out} \rangle + \langle (P_T^{\,2})_{in} \rangle \tag{22}$$

From the distributions of these "in" and "out" components for $E_{c.m.} = 27.4\text{-}31.6$ GeV of the TASSO experiment[39]. We find

$$\langle (P_T^{\,2})_{out} \rangle = 0.057 \text{ GeV}^2, \quad \langle (P_T^{\,2})_{in} \rangle = 0.226 \text{ GeV}^2.$$

Note that the "out" component is much smaller than the "in" component, indicating that the ellipsoid is rather flattened, in contrast with the case of $e^+e^- \to q\bar{q}$ without gluon emission for which the ellipsoid is of revolution around the n_3 axis.

To investigate further the properties of P_T in this case of $e^+e^- \to q\bar{q}g$ we have plotted in Fig. 10 log of $d\sigma/dP_T^{\,2}$ divided by $\sqrt{m_T}$ against $m_T = \sqrt{P_T^{\,2} + m^2}$. We note that for $m_T \lesssim 0.9$ GeV, i.e. $P_T \lesssim 0.89$ GeV/c, the behavior is linear as shown by the least-squares fit, whereas there is a systematic deviation for $P_T > 0.9$ GeV/c, as expected from mesons produced by gluon fragmentation. From the slope of the fitted straight line we obtain a temperature $T = 141 \pm 4$ MeV

corresponding to $\langle P_T \rangle = 348 \pm 12$ MeV/c, compared to $\sim 430 \pm 20$ MeV/c for 2-jet events at 27.4 GeV measured by the PLUTO collaboration.[21] This indicates that most gluons are rather soft as expected from bremsstrahlung.

Finally, we mention the relationship between $\langle P_T^2 \rangle$ and T according to the Bose-Einstein distribution as follows:

$$\langle P_T^2 \rangle = 2mT \frac{K_3(m/T)}{K_2(m/T)} . \tag{23}$$

A plot of $\langle P_T^2 \rangle$ vs. T is shown in Fig. 11. Note that in the high energy limit, $x = m/T$ is small and that we may approximate [40]

$$K_n(x) \simeq \tfrac{1}{2}\Gamma(n)(2/x)^n \tag{24}$$

Γ being the factorial function, so that

$$< P_T^2 > \simeq 8\ T^2 \tag{25}$$

Thus, in view of the empirical power law (14) between T and $E_{c.m.}$ we may write $< P_T^2 > \sim E_{c.m.}^a$ (26)

From the TASSO data of $< P_T^2 >$ from 13 to 31.6 GeV,[41] Fig. 12, we find $a = 0.41 \pm 0.06$, indicating that the increase of $< P_T^2 >$ with $E_{c.m.}$ is much slower than the QCD prediction [42]

$$<P_T^2> \sim E_{c.m.}^2 / \ell n(E_{c.m.}/\Lambda) \tag{27}$$

Λ being the mass scale, see Eq. (3). Furthermore, according to (27), the curvature is upward instead of downward as shown by the data in Fig. 12.

Appendix III

In the present analysis of the transverse momentum P_T, we have used the Bose-Einstein distriubtion, Eq. (10), instead of the Gaussian distribution

$$\frac{d\sigma}{dP_T^2} \sim e^{-P_T^2/2\sigma^2} \tag{28}$$

Note that both distributions involve only one parameter. Consequently, by means of a judicious combination of $\langle P_T \rangle$ and $\langle P_T^2 \rangle$, we may eliminate the parameter and obtain a relation to test the validity of these distributions.

Indeed, from the well known Gaussian distribution, namely

$$\langle P_T \rangle = \sqrt{\pi/2}\sigma, \quad \langle P_T^2 \rangle = 2\sigma^2 \tag{29}$$

it is readily seen that

$$\left(\frac{\sqrt{\langle P_T^2 \rangle}}{\langle P_T \rangle}\right)_G = \frac{2}{\sqrt{\pi}} = 1.13. \tag{30}$$

As for the Bose-Einstein distribution, we may derive an approximate closed form by substituting (24) into Eq. (13) of $\langle P_T \rangle$. We then obtain

$$\left(\frac{\sqrt{\langle P_T^2 \rangle}}{\langle P_T \rangle}\right)_{B.E.} \simeq \frac{8\sqrt{2}}{3\pi} = 1.20 \tag{31}$$

We have checked this result with numerical calculations of $\langle P_T \rangle$ and $\langle P_T^2 \rangle$ according to Eqs. (13) and (23), and found that (31) is accurate within $\sim 1\%$.

We now apply the test with the experimental data of the TASSO collaboration.[41] The result is shown in Fig. 13. The average

$$\left(\frac{\sqrt{\langle P_T^2 \rangle}}{\langle P_T \rangle}\right)_{exp.} = 1.24 \pm 0.05 \tag{32}$$

is shown by the straight line. A comparison with the expected value in (30) and (31) indicated a better accord with the Bose-Einstein distribution. The same conclusion has been reached with P_T distributions of pions from pp and πp collisions, and $\bar{p}p$ annihilation, Ref. 8 (a). This justifies a posteriori our preference to the Bose-Einstein distribution.

Finally, we mention another advantage of the Bose-Einstein distribution, namely the temperature T defined by the P_T distribution is found to be independent of the mass m of the particle in the case of mesons produced by hadron-hadron collisions[36], indicating that T is the equilibrium temperature, a property to be investigated with e^+e^- annihilations when data will be available.

References and Footnotes

1. For a survey on this subject, we refer to G. Wölf, Selected Topics on e^+e^- Physics, DESY 80/13.
2. See R.F. Schwitters and K. Strauch, Ann. Rev. Nucl. Sc. 26, 89 (1976).
3. As is well known, ℓns represents essentially the longitudinal phase space. It is often used for the energy dependence of the average multiplicity, in the spirit of "ℓns Physics"; see M. Jacob, Comments on Nucl. and Part. Phys. V1A, 133 (1976).
4. R. Feynman, Phys. Rev. Lett. 23, 1415 (1969).
5. E.V. Shuryak, Phys. Lett. 34B, 509 (1971); M. Chachian, H. Satz, and E. Suhonen, Phys. Lett. 50B, 362 (1974); E.L. Feinberg, Phys. Lett. 52B, 203 (1974); F. Cooper and G. Frye, Phys. Rev. 11D, 192 (1975); and V. Cannuto J. Lodenquai, Phys. Rev. 11D, 233 (1975).
6. J.D. Bjorken and S.J. Brodsky, Phys. Rev. 1D, 1416 (1970); and J. Engels, K. Schilling, and H. Satz, Nuovo Cimento, 17A, 535 (1973).
7. G.G. Hanson et al., Phys. Rev. Lett. 35, 1609 (1975).
8. T.F. Hoang, Nucl. Phys. B38, 333 (1972); Phys. Rev. D6, 1328 (1972); D8, 2315 (1973); and D12, 296 (1975).
9. Roma-Bologna-Frascati collaboration, C. Bacci et al., Phys. Lett. 86B, 234 (1979).
10. SPEAR, see G.G. Hanson, 13th Rencontre de Moriond (1978), ed. J. Tran Thanh Van, vol. II, p. 15; DASP collab, R. Brandelik et al., Nucl. Phys. B148, 189 (1979); PLUTO collab, Ch. Berger et al., Phys. Lett. 81B, 410 (1979); and TASSO collab, R. Brandelik et al., Phys. Lett. 89B, 418 (1980).
11. W. Furmanski, R. Petronzio, and S. Pokorski, Nucl. Phys. B155, 253 (1979); A. Basseto, M. Ciafaloni, and G. Marchesini, Phys. Lett. 85B, 207 (1974); and K. Konischi, Rutherford, 79-035 (1979), and CERN TH 2897 (1980).

12. The scale constant Λ has been estimated from neutrino charged-current interactions; see CERN-Dortmund-Heidelberg-Saclay-Bologna collaboration, F. Eiselle et al., Phys. Lett. 82B, 456 (1979).

13. L.D. Landau, Izv. Akad. Nauk. SSR 17, 59 (1953); and S.Z. Belen'kji and L.D. Landau, Suppl. Nuovo Cimento 3, 15 (1956).

14. We recall that Landau's model treats the mesons as a photon gas, for which the chemical potential is $\zeta = \varepsilon - Ts + p = 0$ where ε is the energy per unit volume, T the temperature, s the entropy per unit volume and p the pressure (see Ref. 13). Noting that the sound velocity is defined by $c_s^2 = p/\varepsilon$, we find as in Landau's work

$$s \sim \varepsilon^{1/(1+c_s^2)}$$

and for the total entropy

$$S = sV \sim E_{c.m.}^{1/(1+c_s^2)} V^{1-1/(1+c_s^2)},$$

which leads to Eq.(4), assuming $\langle n \rangle$ to be proportional to S and V to be a constant. Note that for $c_s^2 = 1/3$ and V is Lorentz contracted, i.e. $V = V_o/E_{c.m.}$ we find $S \sim E_{c.m.}^{1/2}$ which is Landau's original result from meson production by nucleon-nucleon collisions.

15. It has been pointed out to us by Prof. T. O'Halloran that the SPEAR data of $\langle n_{ch} \rangle$ corrected for heavy leptons are actually $\sim$8% higher--see J. Siegrist, SLAC publ 225 (1979)--and gives better agreement with our fit.

16. JADE collaboration, W. Bartel et al., Phys. Lett. 88B, 171 (1979).

17. T.F. Hoang et al., Phys. Rev. Lett. 27, 1681 (1971), and Ref. 8 (a), (b), and (d).

18. See Ref. 10 (a). We thank Dr. Hanson for providing us with the data used in the present work.

19. We recall that λ describes the anisotropy of the c.m. angular distribution of the emitted mesons, and that $\lambda = 1$ corresponds to an isotropic angular distribution. In other words, λ is essentially related to the velocity of the fireball in the c.m.s. For a detailed description, we refer to Ref. 8(c) and (d).

20. The values of λ and T are taken from a previous study on pp inclusive reactions; see Ref. 8(b)-(d).

21. PLUTO collaboration, Ch. Berger et al., Phys. Lett. 78B, 176 (1978). It should be mentioned that this "on-resonance" point has been excluded because we are only concerned with the continuum.

22. We have used the data form from J.L. Siegrist, SLAC-225 (1979), p. 84, and G.J. Feldman and M.L. Perl, Phys. Rep. 33, 285 (1977). We note that there is a systematic deviation between the data of SLAC and PETRA. See also G. Wölf, loc. cit., p. 124 and G. Hanson, Ref.10 (a).

23. PLUTO collaboration, Phys. Lett. 82B, 449 (1979).

24. See e.g., K. Koller, H. Kraseman, and T.F. Walsh, Z. Phys. C1,71 (1979).

25. DASP collaboration, W. Braunschweig et al., Phys. Lett. 67B, 243 (1977).

26. See Ref. 8(c) for pp, and T.F. Hoang et al., Phys. Rev. D20, 692 (1979) for $\pi^+ p$ and $K^+ p$.

27. See, v.g., F. London, Superfluids, Dover Publications, N.Y. (1964), vol. I, p. 22.

28. For the scaling property of $\bar{p}p$ annihilation, see T.F. Hoang et al., Phys. Rev. D17, 927 (1978).

29. See v.g., R.D. Field and R.P. Feynmann D15, 2590 (1977).

30. F.E. Taylor, Phys. Rev. D14, 1217 (1976).

31. The values of $\langle E_{ch} \rangle / E_{c.m.}$ are taken from the review article by R.F,

Schwitters and K. Strauch, loc. cit., and the values of $\langle n_{ch} \rangle$ are from J. Siegrist, SLAC publ. 225 (1979); see ref. 15.

32. See v.g. F. Karsch and H. Staz, Phys. Rev. D 22, 480 (1980) and references of other works therein.

33. J.I. Kapusta, Nucl. Phys. B148, 461 (1979); and O.K. Kalashnikov and V.V. Klimov, Phys. Lett. 88B, 328 (1979).

34. We thank Prof. G. Trilling for a critical discussion on this problem.

35. The evidence of gluon bremsstrahlung has been reported by several PETRA experiments: TASSO collaboration, R. Brandlick et al., Phys. Lett. 86B, 243 (1979); MARK J collaboration, D.P. Barber et al., Phys. Rev. Lett. 43, 830 (1979); PLUTO collaboration, Ch. Berger, Phys. Lett. 86B, 418 (1979); and JADE collaboration, W. Bartel, Phys. Lett. 91B, 142 (1980).

36. See v.g. T.F. Hoang et al., Phys. Rev. D19, 1468 (1979). We note that the fact that P_T follows the Bose-Einstein distribution requires thermal equilibrium.

37. See v.g. Sau Lan Wu and G. Zobernig, Z. Phys. C2, 107 (1979).

38. TASSO collaboration, R. Brandelik, Phys. Lett. 86B, 243 (1979).

39. The data here used are taken from Figs. 11-21 of Wölf's review article, loc. cit.

40. See N.G. Handbook of Mathematical Functions, Ed. M. Abramowitz, and and I.A. Stegnn, National Bureau of Standards, Washington, D.C. (1964), p. 375.

41. The TASSO data here used are taken from Fig. 11.8 of Wölf's Review paper, loc. cit.

42. See v.g. Konishi (1980), "Status of (QCD Based Understanding of) Jets", Ref. 11.

Figure Captions

1. Average charged multiplicity from e^+e^- annihilations. Data from Ref. 10. The curve is the fit with $\langle n_{ch} \rangle = (0.15 \pm 0.43) + (2.0 \pm 0.04) E_{c.m.}^{1/2}$.

2. Plot of log of $d\sigma/dP_T^2$ divided by $\sqrt{m_T}$ vs. $m_T = \sqrt{P_T^2 + m^2}$ for mesons from e^+e^- annihilation at 7.4 GeV. Data from Ref. 18. The straight line represents the fit with the Bose-Einstein distribution, Eq. (10).

3. Longitudinal momentum distribution of mesons from $e^+e^- \rightarrow$ hadrons. Same data as Fig. 2. The dashed line is the fit with the distribution (11).

4. Relationship between the average momentum and the temperature according to the Bose-Einstein distribution, Eq.(13) for m = 140 MeV.

5. Log plot the energy dependence of the temperature. Data from the PLUTO and the TASSO collaborations, Ref. 10. The straight lines are least-squares fits with a power law; see text.

6. Scaling behavior of $e^+e^- \rightarrow$ hadrons. $\lambda = 2\langle P_T \rangle / \pi \langle P_L \rangle$ is the scaling parameter. The scaling requires $\lambda\sqrt{s}/2$ to be independent of the c.m. energy $\sqrt{s}$.

7. Plots of $1/\lambda$ vs. T. (a) e^+e^- annihilations for $E_{c.m.}$ = 3 to 31.6 GeV and (b) pp collisions for P_{lab} = 12 to 1600 GeV. Note the striking difference between the two plots.

8. Plots of the derivative of $1/\lambda$ with respect to T, same data as Fig. 7. Note the anomaly in the e^+e^- case near $\Upsilon(9.5)$ threshold.

9. Behavior of the ratio of the average energy of the secondary meson to the c.m. energy of e^+e^- annihilation, according to the Bose-Einstein distribution modified for the scaling, using parameters from PLUTO and TASSO collaborations. Open circles are test points from SLAC-LBL data.

10. Plot of log of $d\sigma/dP_T^2$ divided by $\sqrt{m_T}$ vs. $m_T = \sqrt{P_T^2 + m^2}$ for TASSO data at $E_{c.m.}$ = 27.4 - 30 GeV, ref. 38. See text in Appendix II.

11. Plot of $\langle P_T^2 \rangle$ against the temperature according to the Bose-Einstein distribution, Eq. (23) for m = 140 MeV.

12. Energy dependence of $< P_T^2 >$. TASSO data, Ref. 42. The dashed line is a fit with $E_{c.m.}^{0.41}$.

13. Plot of $\sqrt{< P_T^2 >} / < P_T >$ of TASSO data, Ref. 41. The average 1.24 ± 0.05 shown by the straight line is to compare with 1.13 and 1.20 according to the Gaussian and the Bose-Einstein distribution, respectively, see Eqs. (30) and (31).

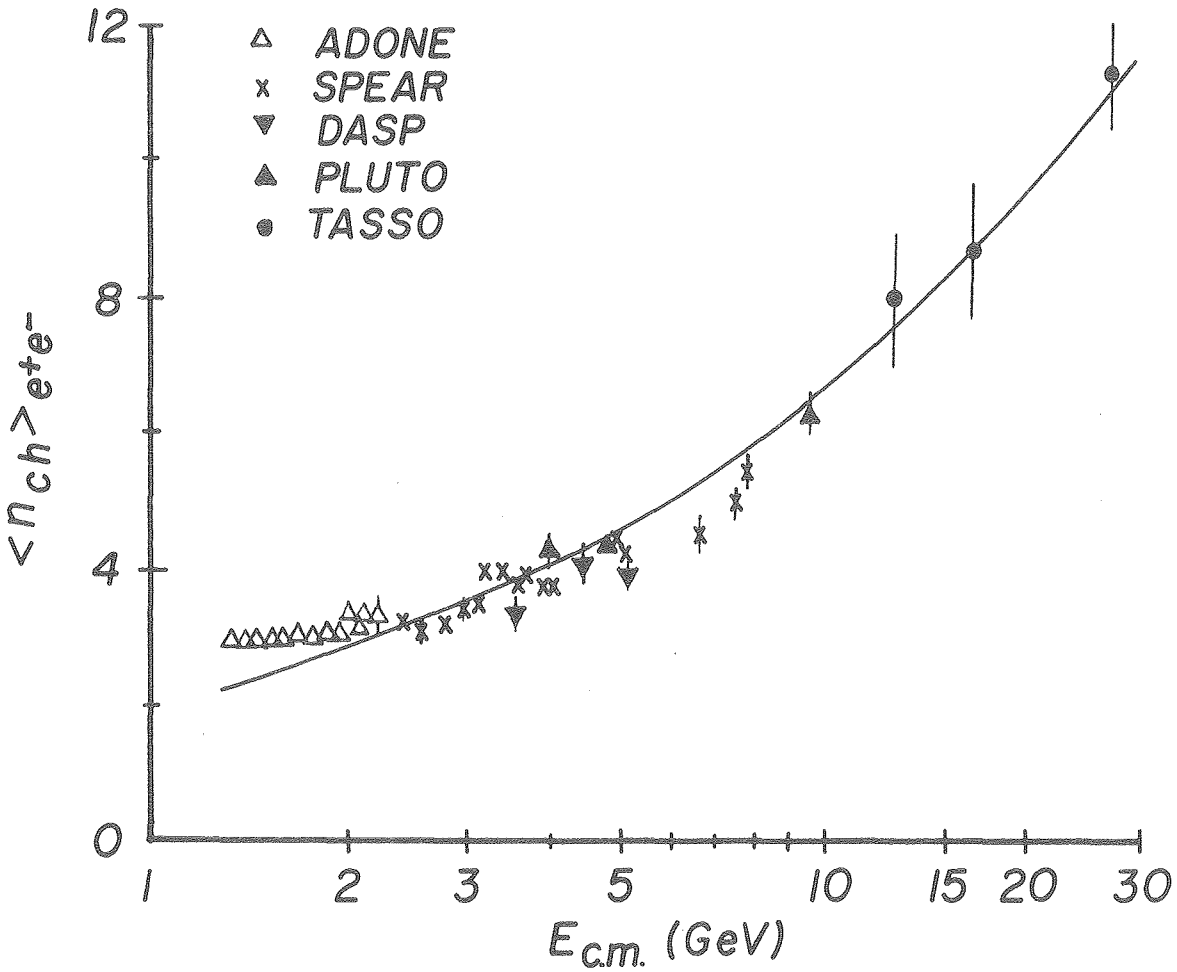

Fig. 1

XBL 7911-12825

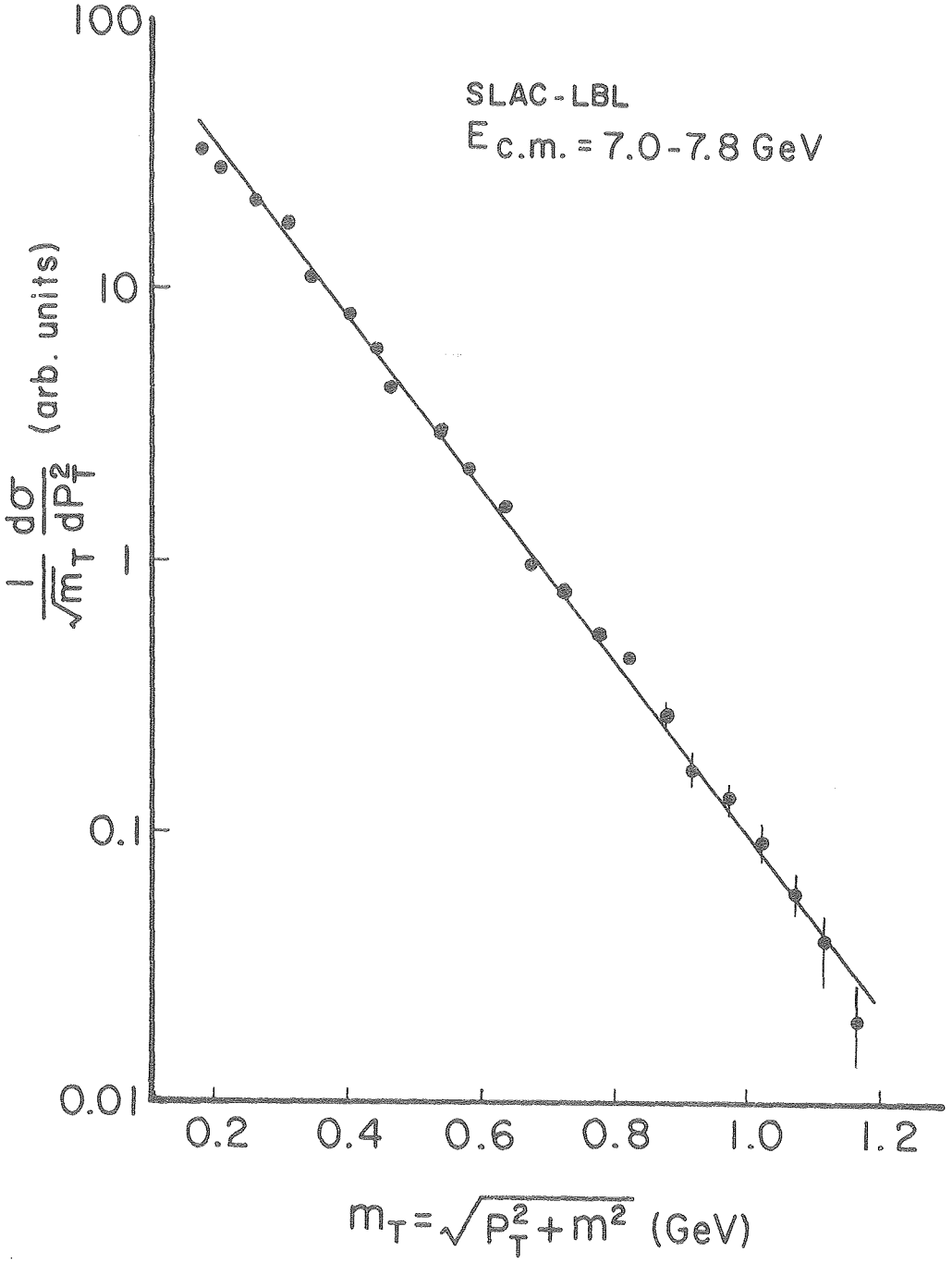
SLAC-LBL
E c.m. = 7.0-7.8 GeV
100
10
1
0.1
0.01
$\frac{1}{\sqrt{m_T}} \frac{d\sigma}{dP_T^2}$ (arb. units)
0.2
0.4
0.6
0.8
1.0
1.2
$m_T = \sqrt{P_T^2 + m^2}$ (GeV)
XBL 8011-3908

Fig. 2

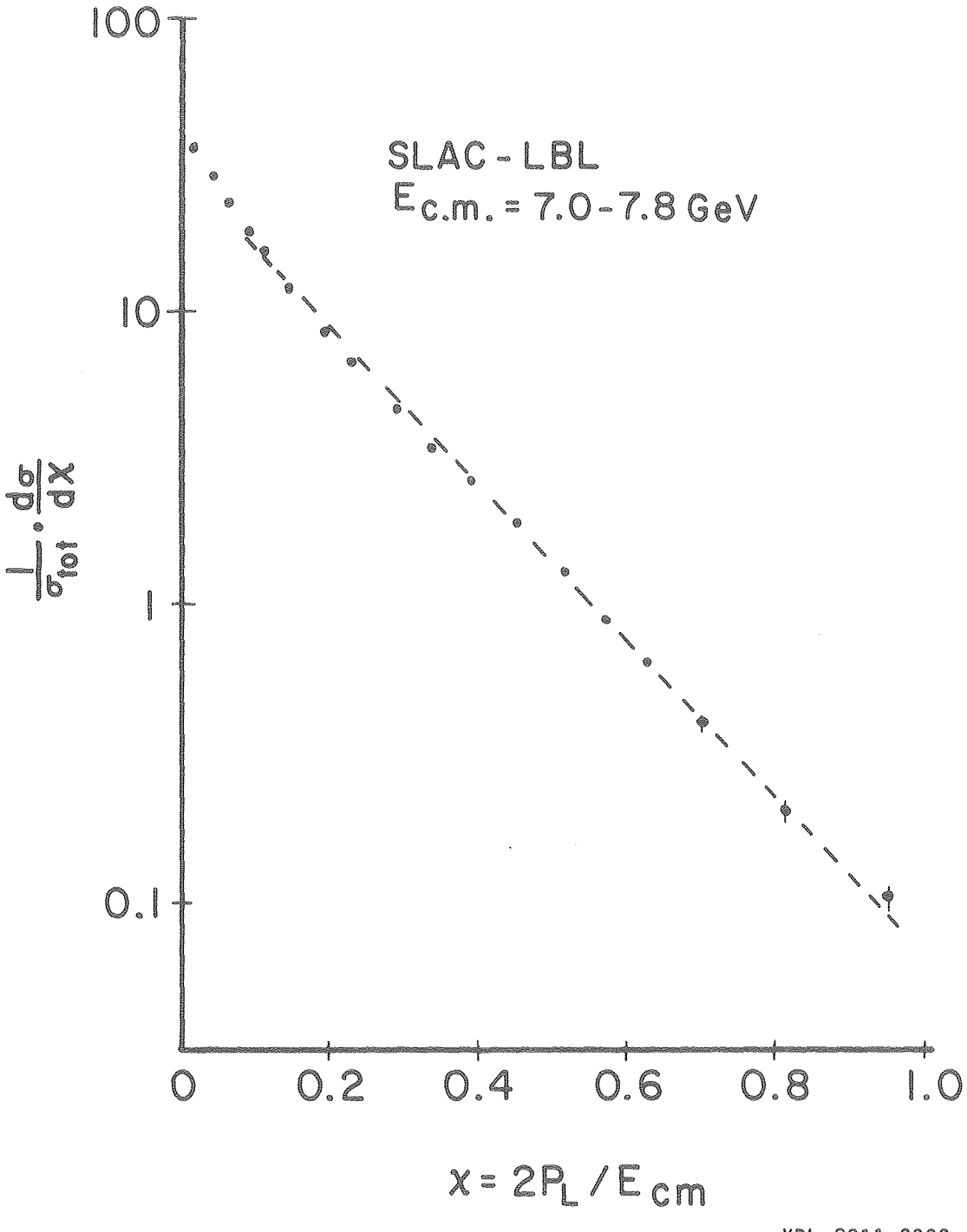
100
10
1
0.1
SLAC - LBL
$E_{c.m.} = 7.0 - 7.8$ GeV
$\frac{1}{\sigma_{tot}} \cdot \frac{d\sigma}{dx}$
0
0.2
0.4
0.6
0.8
1.0
$x = 2P_L / E_{cm}$
XBL 8011-3909

Fig. 3

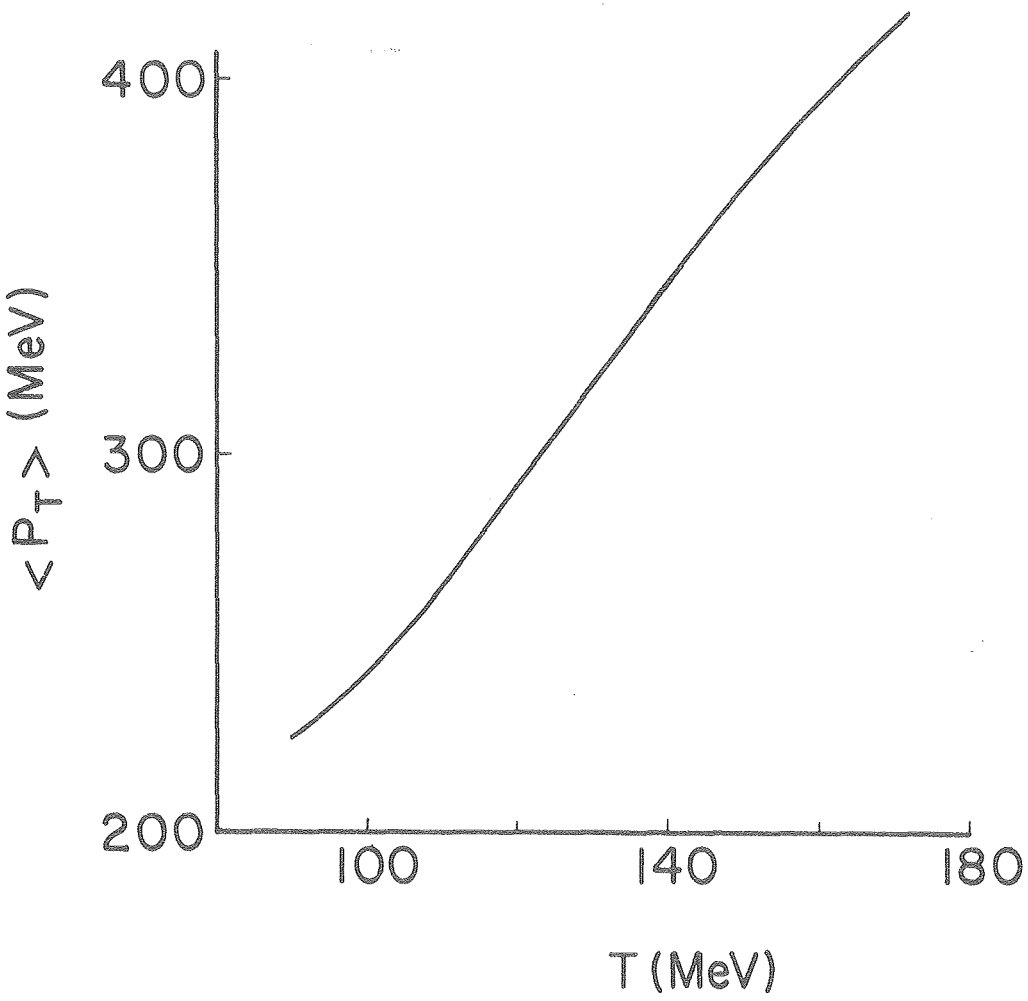

XBL 8011-3910

Fig. 4

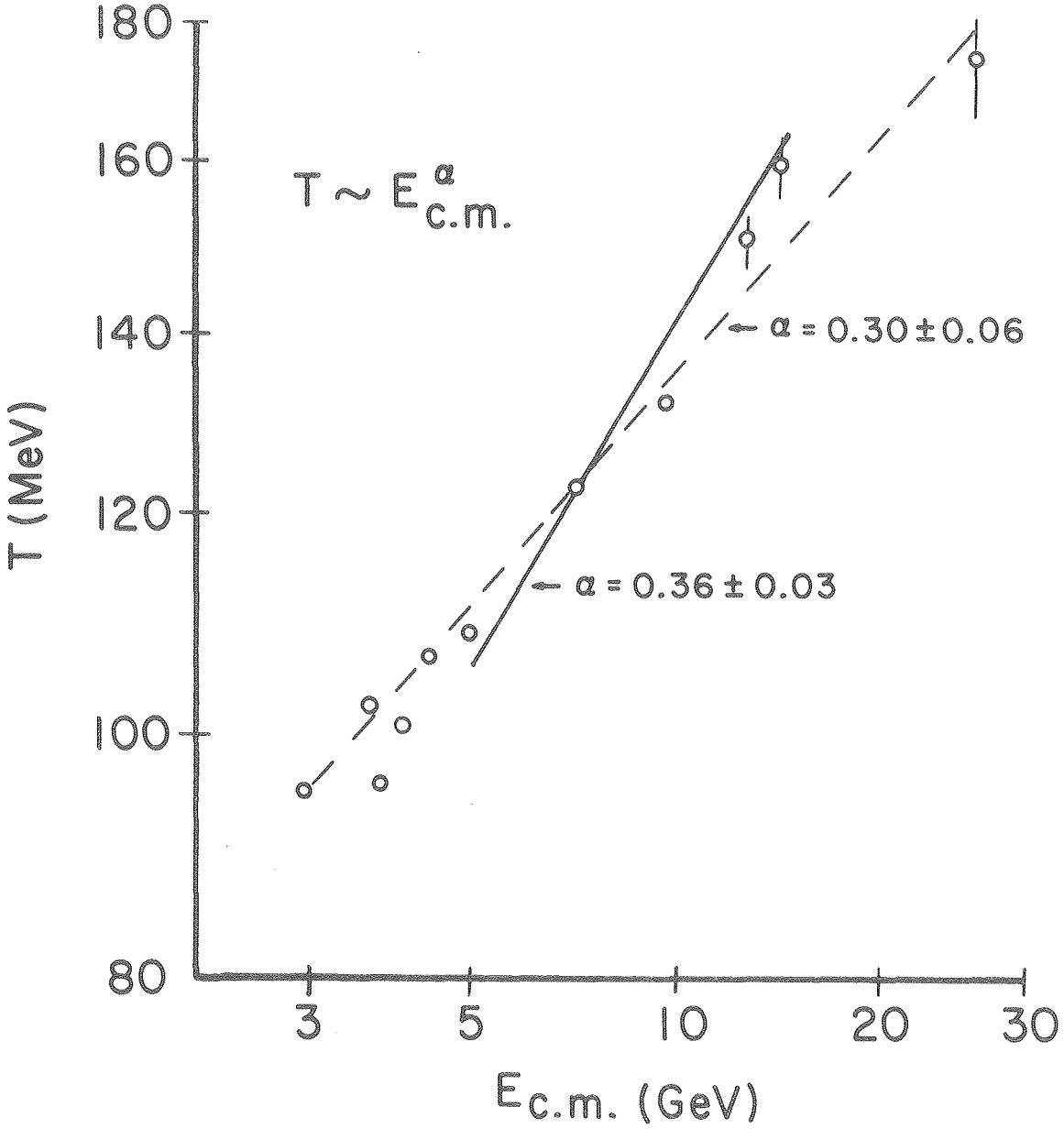
180
160
140
120
100
80
T (MeV)
$T \sim E^{\alpha}_{c.m.}$
$\alpha = 0.30 \pm 0.06$
$\alpha = 0.36 \pm 0.03$
3
5
10
20
30
$E_{c.m.}$ (GeV)
XBL 8011-3911

Fig. 5

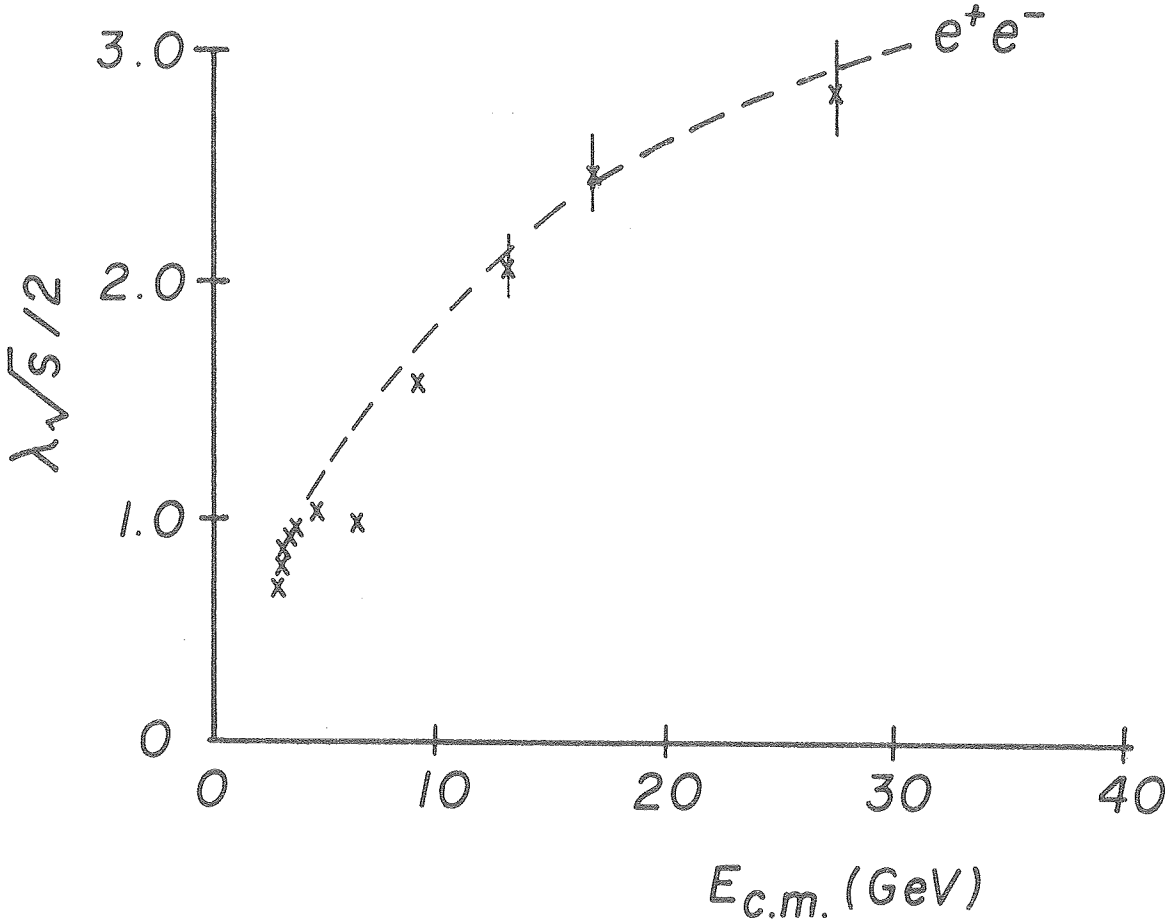

XBL 8011-3912

Fig. 6

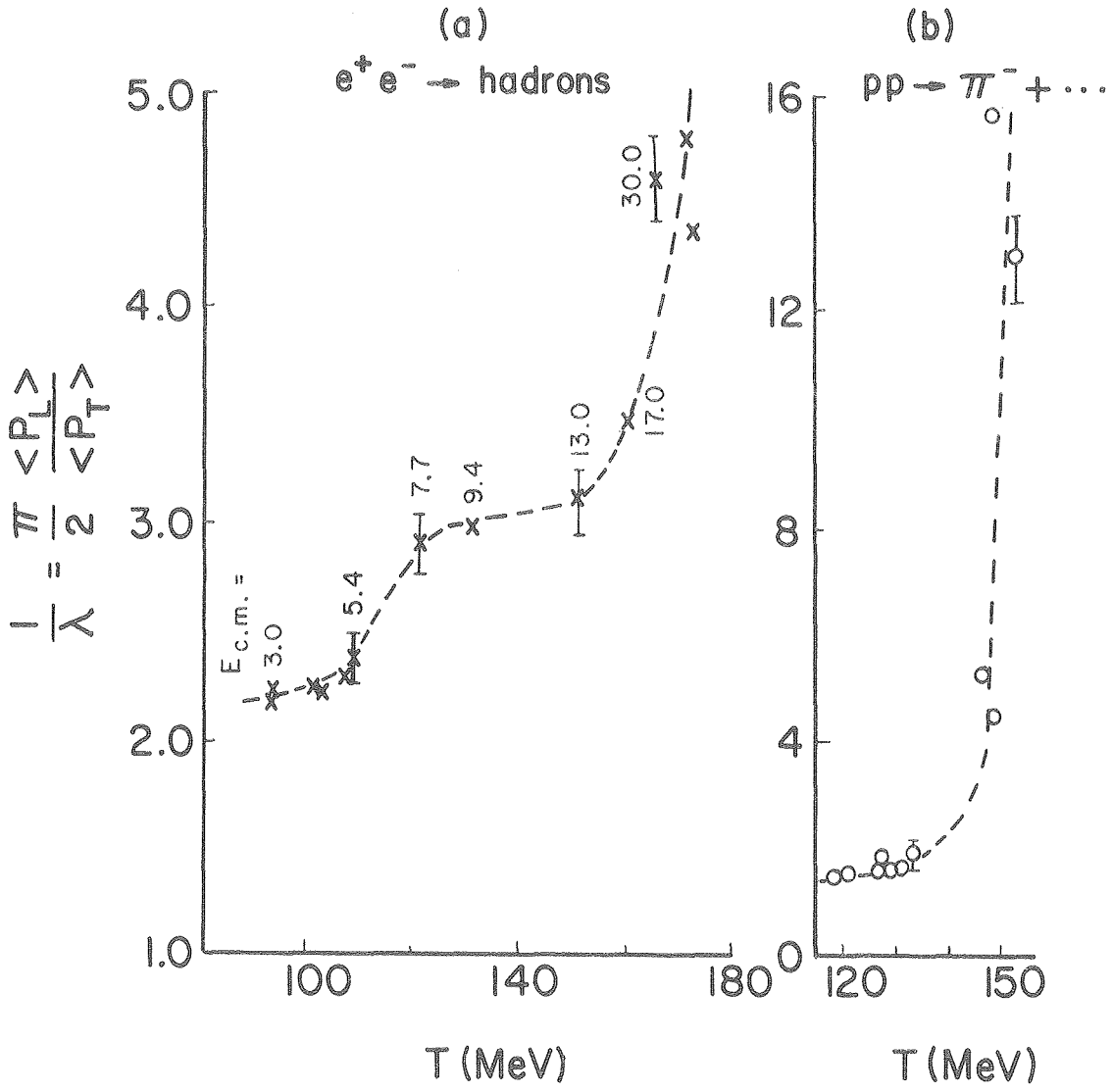

XBL 8011-3913

Fig. 7

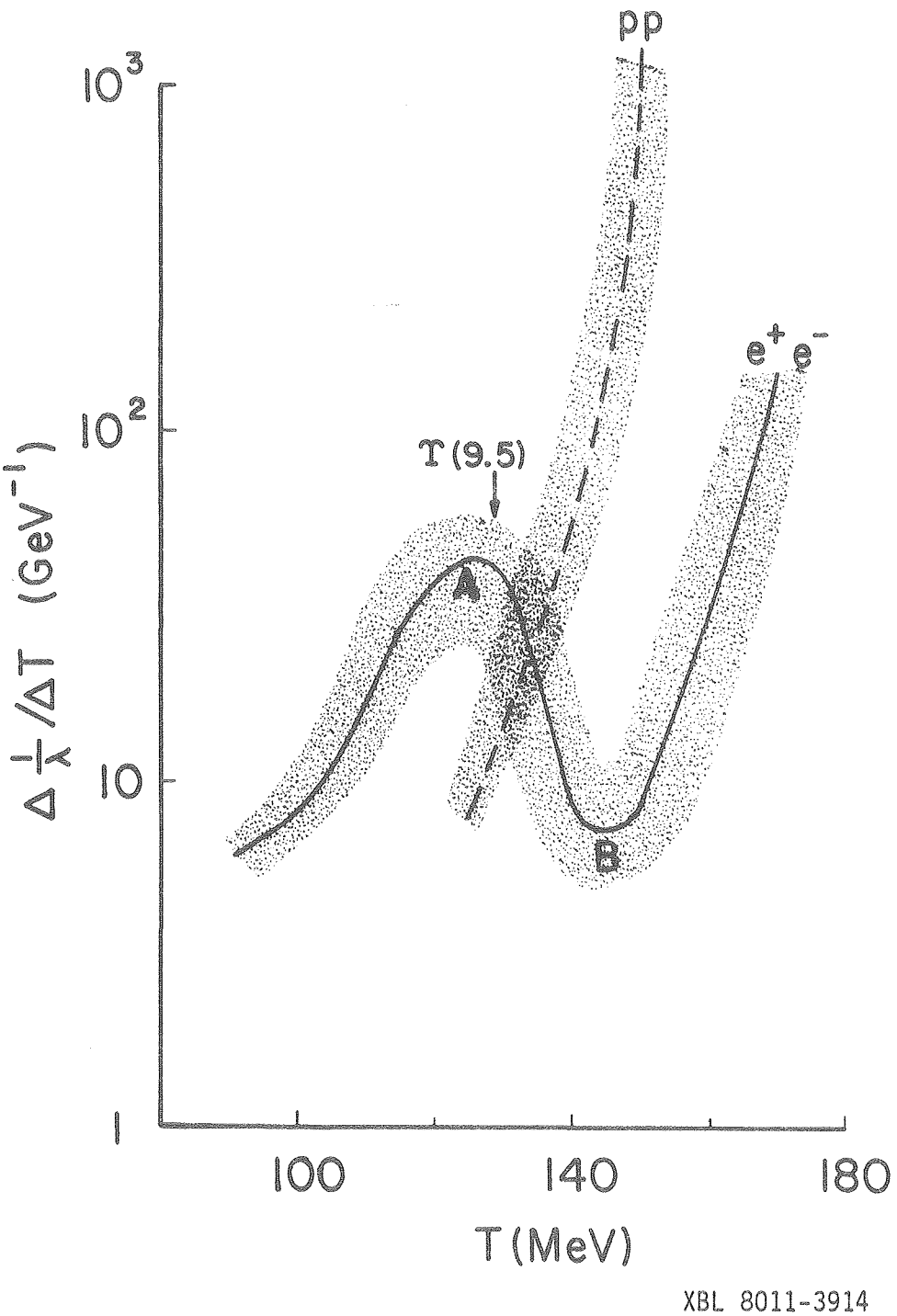

XBL 8011-3914

Fig. 8

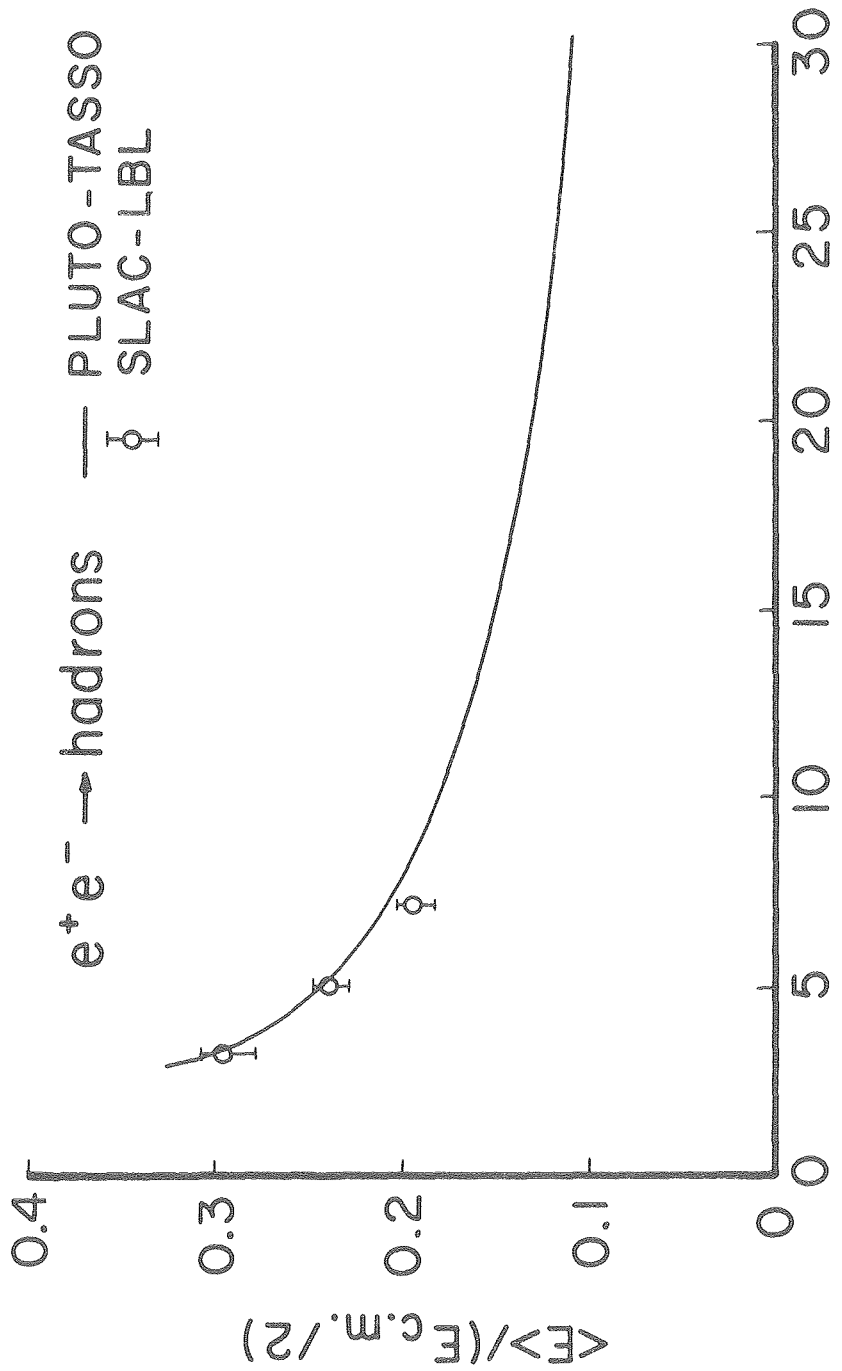
$e^+e^- \rightarrow$ hadrons
PLUTO-TASSO
SLAC-LBL
$\langle E \rangle / (E_{c.m.}/2)$
$E_{c.m.}$ (GeV)
0.4
0.3
0.2
0.1
0
5
10
15
20
25
30
XBL 8011-3915

Fig. 9

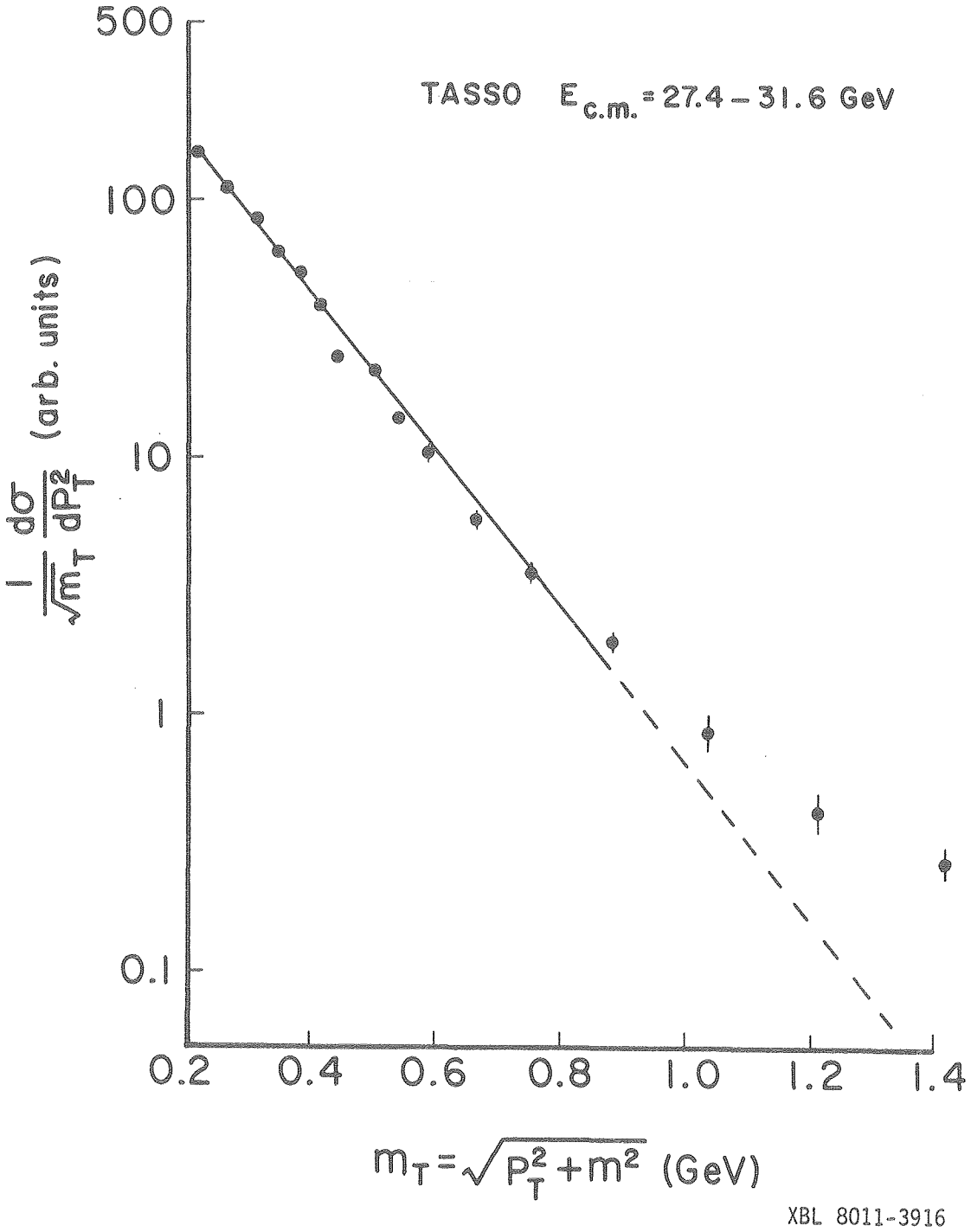
TASSO $E_{c.m.} = 27.4 - 31.6$ GeV
500
100
10
1
0.1
$\frac{1}{\sqrt{m_T}} \frac{d\sigma}{dP_T^2}$ (arb. units)
0.2
0.4
0.6
0.8
1.0
1.2
1.4
$m_T = \sqrt{P_T^2 + m^2}$ (GeV)
XBL 8011-3916

Fig. 10

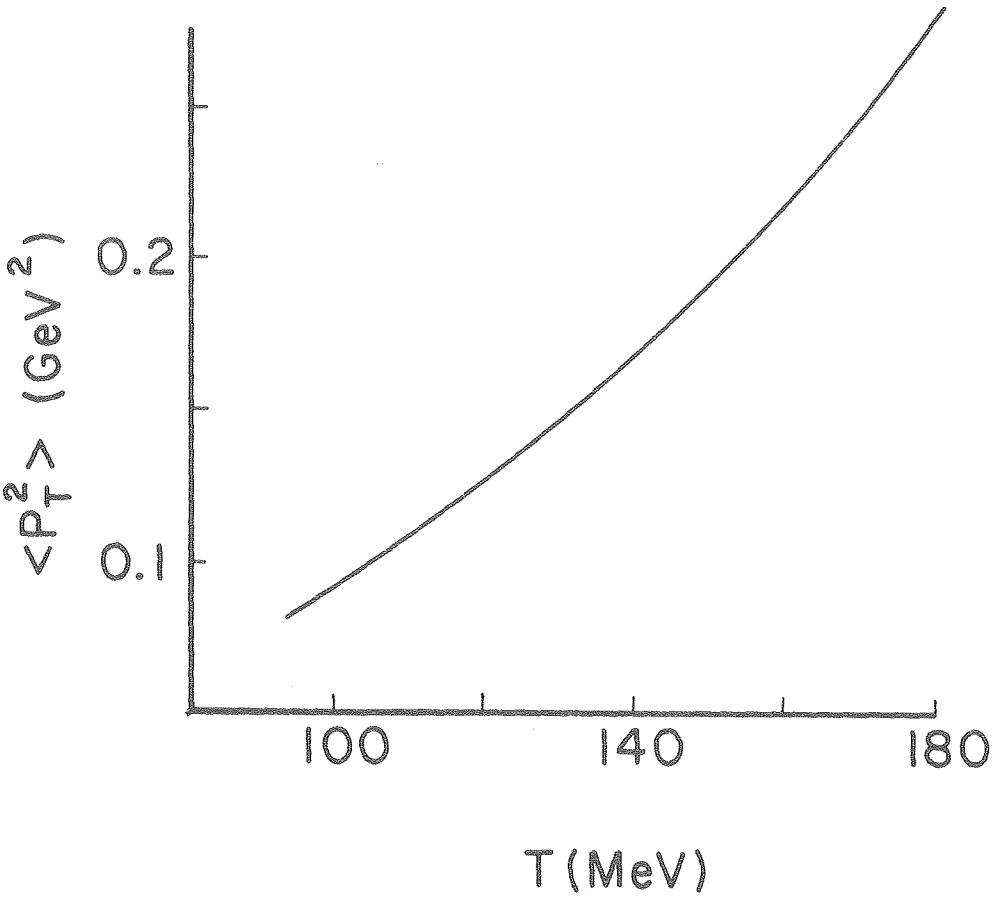

XBL 8011-3917

Fig. 11

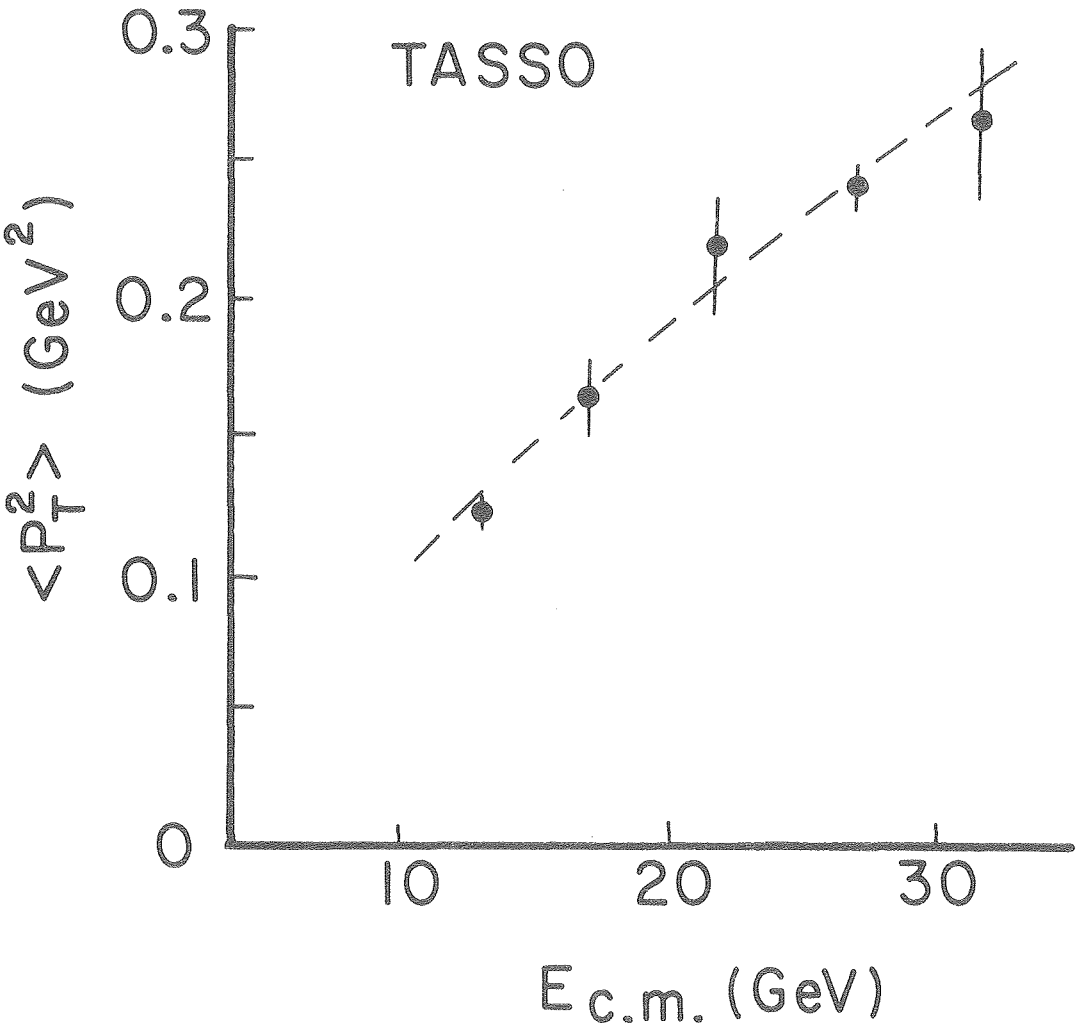

XBL 8011-3918

Fig. 12

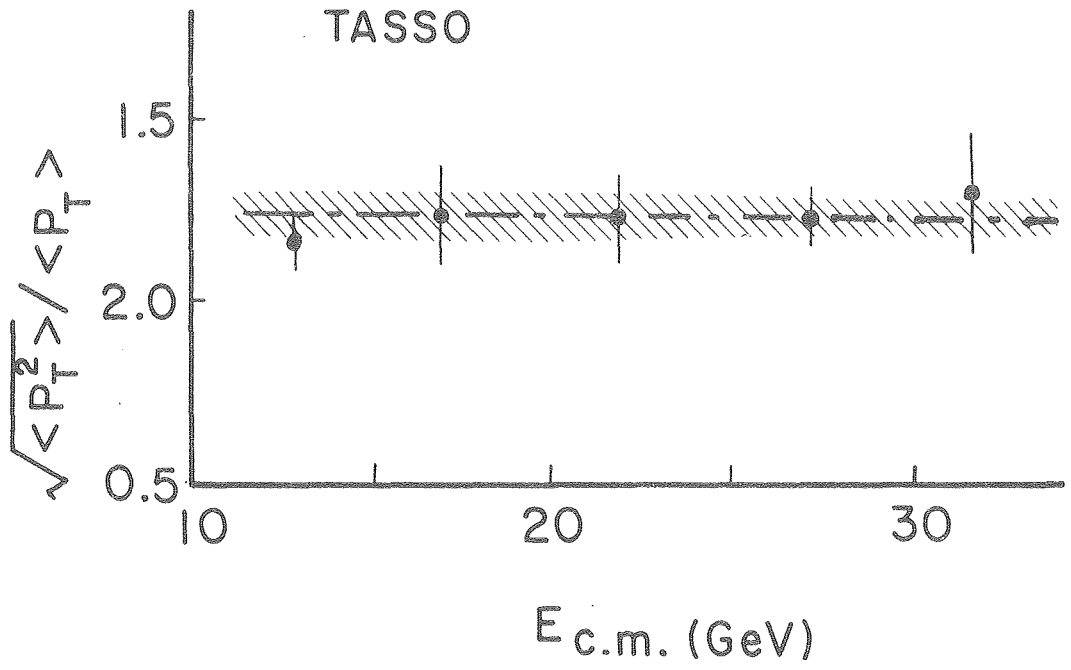

XBL 8011-3942

Fig. 13